ISSN- 0102-9010

# MORPHOMETRIC ANALYSIS AND ULTRASTRUCTURE OF THE EPITHELIUM OF THE ORAL MUCOSA IN DIABETIC AUTOIMMUNE NOD MICE

Eduardo José Caldeira[1], Progresso José Garcia[2], Elaine Minatel[1], José Angelo Camilli[1], Valéria Helena Alves Cagnon[1]

[1]Department of Anatomy, Institute of Biology, State University of Campinas (UNICAMP), Campinas, SP, Brazil.
[2]Department of Anatomy, Institute of Biosciences, Paulista State University (UNESP), Botucatu, SP, Brazil.

## ABSTRACT

Several studies have examined the deleterious effects of diabetes on the oral mucosa. In this study, we examined the histological, ultrastructural and stereological changes in the oral epithelium of diabetic NOD mice and correlated the findings with the processes of tissue repair, healing and susceptibility to infection. Twenty-seven female mice were allocated to one of three experimental groups (n= 9/ group) BALB/c control mice, non-diabetic NOD mice and diabetic NOD mice. After confirmation of the diabetic state based on the urine glucose levels, tissue samples were collected from the cheek mucosa and processed for light and transmission electron microscopy. Diabetic NOD mice showed atrophy of the oral epithelium with definite cellular polymorphism and indistinguishable cell layers. The alterations seen included a reduced number of cell organelles, cell membrane disorganization, the accumulation of lipid droplets in the cell cytoplasm, an increased intercellular space and slight superficial desquamation. Non-diabetic NOD mice showed only moderate morphological alterations in the cheek mucosa. These results indicate that diabetes adversely affects the morphology of the cheek mucosa, which may compromise tissue function to favor the occurrence of oral infections.

**Keywords:** Autoimmune diabetes, oral mucosa, ultrastructure

## INTRODUCTION

Diabetes mellitus is a chronic disease that produces severe metabolic disorders. The main characteristic of diabetes is hyperglycemia, which results from poor glucose use because of insufficient insulin secretion and hepatic gluconeogenesis [7,33]. Type I or insulin-dependent diabetes affects approximately 10% of diabetic patients in the western world [37]. This type of diabetes results from a lack of insulin caused by autoimmune destruction of the pancreatic beta cells [18]. Various studies have established diagnostic criteria to help elucidate the etiology of diabetes and its deleterious effects in a variety of organs, including the vascular, renal, ophthalmic, neurological, digestive and reproductive systems [1,2,4,10,12,37]. An association between diabetes mellitus and alterations in the oral mucosa has been observed in experimental studies and clinical practice, and includes changes in the healing process of lesions as well as the triggering of infectious processes in the mucosal lining [11,13,17]. In addition, studies in alloxan-induced diabetic rats have shown a marked decline in the rate of cell proliferation in the oral mucosa, an increase in the lactobacillus flora and the presence of caries and periodontal disease [16,31]. In streptozotocin-diabetic rats, an important reduction in the tolerance of gingival supporting tissues to continuous mechanical pressure has been reported [27].

The aim of this study was to examine the alterations in the histology and ultrastructure of the oral epithelium of nonobese diabetic (NOD) mice, which have autoimmune diabetes that resembles human type I diabetes [24,38]. We also investigated the correlation between the results obtained and the processes of tissue repair, healing and susceptibility to infection.

## MATERIAL AND METHODS

*Animals and tissue preparation*

Twenty-seven female mice 15 weeks old were allocated to one of three experimental groups (9 mice/ group): BALB/c

Correspondence to: Dr. Valeria H. A. Cagnon
Departamento de Anatomia, Instituto de Biologia, Universidade Estadual de Campinas (UNICAMP), CP 6109, CEP: 13083-970, Campinas, SP, Brasil. Tel: (55) (19) 3788-6102. Fax (55) (19) 3289-3124. E-mail: quitete@unicamp.br

control mice (non-autoimmune and non-diabetic), non-diabetic autoimmune NOD mice and diabetic autoimmune NOD mice 20 days prior to use. The mice were fed standard rodent chow (Nuvilab CR 1), and the food and water intake were quantified daily. Urine glucose and protein levels (mg/dl) were measured in each mouse twice a day using commercial kits (Bayer MultistiK 10 SG). The mice were weighed at the beginning and at the end of the experiment. When required, the mice were anesthetized with Francotar/Virbaxil (1:1/0.25 ml/100g body weight) and sacrificed by anesthetic overdose. For light microscopy, samples of cheek mucosa from four mice in each group were fixed in Bouin solution and embedded in plastic resin (Paraplast Plus). Sections (6 µm thick) were stained with hematoxylin and eosin. Photomicrographs were obtained with a Nikon photomicroscope. For transmission electron microscopy, five mice in each group were perfused with Karnovsky solution [22] and the tissue was immediately removed, fixed in the same solution for 24 h and post-fixed in 1% osmium tetroxide for 2 h. The specimens were then dehydrated, embedded in plastic resin (Polyscience), cut into ultrathin sections with an LKB ultramicrotome and counterstained with uranyl acetate and lead citrate [32,39]. The material was examined and photographed with a LEO-906 transmission electron microscope in the Electron Microscopy Laboratory, in the Institute of Biology, UNICAMP.

*Light microscopy and stereological parameters*

The material processed for light microscopy as described above was used to determine the cytoplasmic and nuclear volumes of the basal cells and the epithelium thickness. Cytoplasmic and nuclear volumes were measured using the point counting method of Weibel [40], with the nuclear volume being determined by measuring the diameter of 50 basal epithelial cell nuclei in the cheek mucosa of each mouse. Epithelium thickness was determined as the mean height of the four regions of oral mucosa in each mouse, and was measured using an ocular grid (10 mm/100, Zeiss) coupled to an Olympus CBB microscope equipped with a 100X lens [40].

*Statistical analysis*

The results were expressed as the mean ± S.D. Body weight variation (final weight minus initial weight), mean diameter of basal epithelial cells nuclear and cytoplasmic volumes, and epithelium thickness were compared using Tukey's mean comparison test [26], followed by a multiple comparison test involving all pairs of groups [28]. The level of significance was set at 1%.

## RESULTS

*Urine analysis*

The mean urine glucose and protein concentration were 30 mg/dl, respectively, for BALB/c and non-diabetic autoimmune NOD mice, compared to 750 mg/dl and 10 mg/dl in the diabetic autoimmune mice throughout the 20 days of the study (n = 9 group).

*Body weight variation*

There was a significant increase in body weight in the BALB/c and non-diabetic autoimmune NOD mice compared to diabetic autoimmune NOD mice during the study (Table 1).

*Light microscopy*

A 9 µm thick keratinized, stratified squamous epithelium was observed in the cheek mucosa of control BALB/c mice (Table 1). This epithelium consisted of basalis, spinosum, granulosum and corneum cell layers with marked epithelial cristae located above a clear basal membrane (Fig. 1A). Columnar cells with a centrally located nucleus were observed in the basal cell layer (Fig. 1A). In the spinosum and granulosum layers, the cells were voluminous and flat, respectively, and had a centrally located nucleus. Superficially, flattened cells in the process of desquamation were identified in the corneum layer (Fig. 1A). The lamina propria consisted of fibroblast cells and other cell types scattered throughout the connective tissue (Fig. 1A). In non-diabetic autoimmune NOD mice, the epithelium had a mean thickness of 4.3 µm (Table 1), occasional epithelial cristae, and basal cells with reduced cytoplasmic and nuclear volumes and impaired stratification of the spinosum, granulosum and corneum cell layers (Fig. 1B and Table 1). Apparent involution and a decrease in cell number were

**Table 1.** Body weight variation, nuclear and cytoplasmic volume of basal cells and thickness of the epithelium in the oral mucosa of Balb/c (control) and NOD mice.

| Variable | Balb/c mice | NOD mice | |
|---|---|---|---|
| | | Non-diabetic | Diabetic |
| Nuclear volume (µm$^3$) | 3.08±0.24(c) | 2.34±0.29(b) | 1.83±0.29(a) |
| Cytoplasmic volume (µm$^3$) | 8.03±0.72(c) | 6.30±0.78(b) | 4.40±0.88(a) |
| Epithelial thickness (µm) | 9.00±0.82(c) | 4.30±0.48(b) | 2.80±0.81(a) |
| Weight variation (g) | 1.20±1.18(a) | 1.60±1.09(a) | -2.40±1.15(b) |

The values are the mean ± S.D. Different letters indicate significant differences (P< 0.01).

observed in the spinosum and granulosum strata, respectively. The corneum layer showed minor desquamation. The lamina propria consisted of fibroblasts and other cell types scattered throughout the connective tissue (Fig. 1B).

In diabetic autoimmune NOD mice, the epithelium was atrophic (mean thickness, 2.8 μm) and the basement membrane had occasional epithelial cristae (Fig. 1C and Table 1). Identification of the different cell layers was difficult. In the basal cell layer, pleomorphic cells with a marked reduction in cytoplasmic and nuclear volumes were observed (Fig. 1C and Table 1). The cells of the spinosum and granulosum layers were apparently involuted, and the corneum layer showed minor desquamation (Fig. 1C). The lamina propria consisted of fibroblastic cells and various cell types scattered throughout the connective tissue (Fig. 1C).

*Transmission electron microscopy*

Ultrastructurally, in control mice, a basal-located nucleus of the basal cells presented an evident nucleolus, and the chromatin was homogenously distributed and condensed close to the nuclear membrane (Fig. 2A,B,C). Spherical and elongated mitochondria were noted in the basal cell cytoplasm. A granular endoplasmic reticulum with flattened and parallel cisternae was located in the perinuclear region (Fig. 2B, Inset). The spinosum cells were voluminous and polyhedral, with an irregular nucleus, homogenously to distributed chromatin and an evident nucleolus (Fig. 2D). The cytoplasm of these cells contained electron-dense spherical granules, mitochondria and a markedly by granular endoplasmic reticulum in the perinuclear region (Fig. 2D). The granulosum layer was characterized by flattened cells with a centrally located nucleus and invagination of the nuclear membrane. The cytoplasm contained spherical granules, mitochondria and a markedly granular endoplasmic reticulum in the

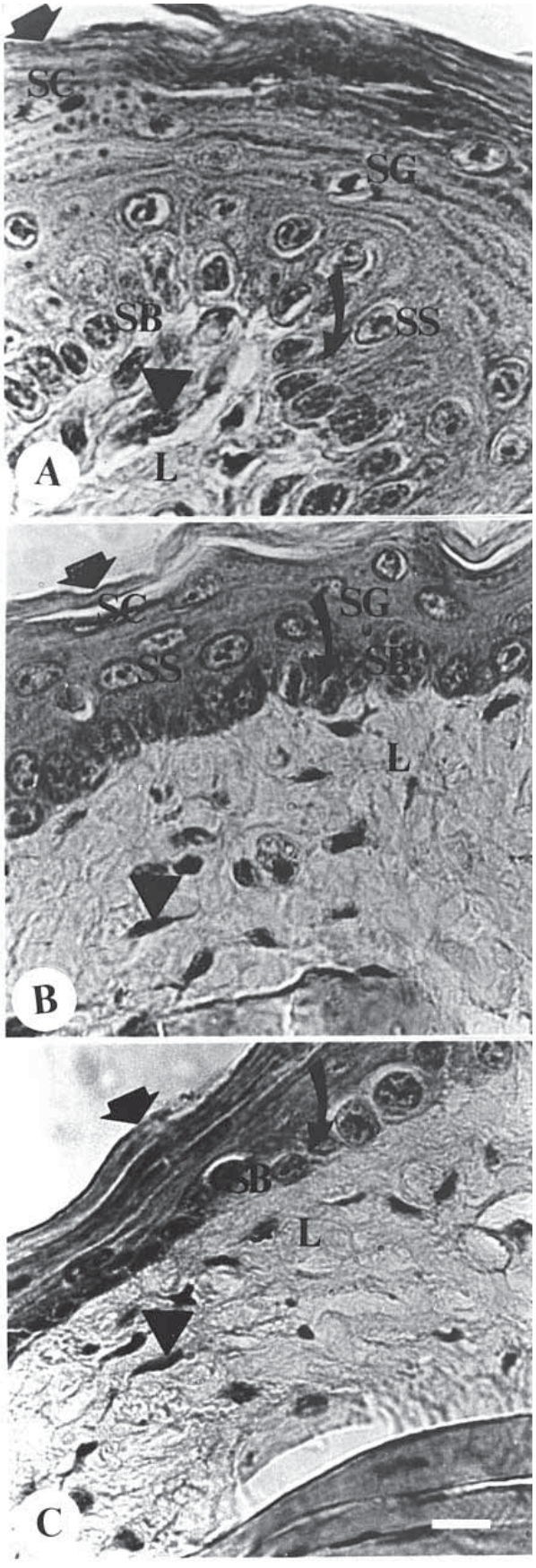


**Figure 1.** Photomicrographs of the oral epithelium of mice. **A:** Balb/c mice: Epithelium showing desquamation (**arrow**), wide epithelial cristae (**curved arrow**), fibroblasts (**arrowhead**) and lamina propria (**L**). Note the epithelial layers, i.e., basal (**SB**), spinosum (**SS**), granulosum (**SG**) and corneum (**SC**) cell layers. H.E. **B:** Non-diabetic NOD mice: Epithelium showing minor desquamation (**arrow**), epithelial cristae (**curved arrow**), lamina propria (**L**) and fibroblasts (**arrowhead**). Reduced epithelium with differentiation of the basal (**SB**), spinosum (**SS**), granulosum (**SG**) and corneum (**SC**) cell layers. H.E. **C:** Diabetic NOD mice: Atypical epithelium with no evidence of epithelial desquamation (**arrow**) and epithelial cristae (**curved arrow**). Atrophic basal cells (**SB**), fibroblasts (**arrowhead**) and lamina propria (**L**). H.E. Bar = 10 μm.

perinuclear region. The cytoplasmic membrane showed indentations and a small intercellular space (Fig. 2E). In the corneum layer, flattened cells in the process of desquamation were noted (Fig. 2F). The lamina propria consisted of connective tissue and transversal and longitudinal collagen fibers (Fig. 2C), in addition to an intact basement membrane at the interface with the lining epithelial (Fig. 2B).

In non-diabetic, autoimmune NOD mice, cellular involution was observed (Table 1) with the nucleus occupying a large part of the cytoplasm and a visible nucleolus and condensed chromatin close to the nuclear membrane (Fig. 3C). Mitochondria and a markedly granular endoplasmic reticulum were observed in the basal region and close to the nuclear membrane (Fig. 3B). Lipid droplets were seen in the basal cytoplasm and desmosomes were also present (Fig. 3A,B, Inset). The spinosum cells were apparently involuted but maintained a polyhedral shape, with an irregular nucleus, condensed chromatin close to the nuclear membrane, and a poorly visible nucleolus (Fig. 3D). The cytoplasm contained small, spherical, electron-dense granules. Mitochondria and a markedly granular endoplasmic reticulum were seen scattered throughout the cytoplasm and in the perinuclear region. An apparent increase in the intercellular space was also noted (Fig. 3D).

In the granulosum layer, the cells apparently involuted with an irregular nucleus occupying a large part of the cytoplasm. The cytoplasm contained electron-dense, spherical granules, probably, keratohyalin granules (Fig. 3E). Superficially, the corneum layer was characterized by flattened cells accompanied by minor desquamation (Fig. 3F). The lamina propria consisted of connective tissue containing transversal and longitudinal collagen fibers (Fig. 3A). An intact basement membrane was located at the interface with the epithelial lining (Fig. 3B).

Diabetic autoimmune NOD mice had a markedly involuted stratified epithelium, with lipid droplets scattered among the basal, spinosum and granulosum layers (Fig. 4A,D). The basal cell layer was characterized by involuted and pleomorphic cells (Table 2), with an irregular nucleus occupying most of the cytoplasm (Fig. 4C). Mitochondria, as well as a granular endoplasmic reticulum with flattened cisternae located in the perinuclear region, were observed in the cytoplasm (Fig. 4B, Inset, and 4C). The intercellular space was markedly increased (Fig. 4B,C). The spinosum cell layer was characterized by cellular involution and pleomorphism (Fig. 4D). The cytoplasm contained electron-dense granules and mitochondria were observed in the perinuclear region; no granular endoplasmic reticulum was seen. The intercellular space was increased (Fig. 4D). The granulosum cell layer was apparently reduced, and contained flattened cells with an irregular nucleus occupying most of the cytoplasm. The cytoplasm of these cells contained spherical, or irregular in shape electrondense granules, probably, keratohyalin granules (Fig. 4E). The corneum layer was characterized by flattened cells lacking a nucleus and organelles. Minor desquamation of the epithelium was observed (Fig. 4F). Transversal and longitudinal colagen fibers were noted in the lamina propria (Fig. 4B), and there was an intact basement membrane at the interface with the epithelial lining (Fig. 4C).

## DISCUSSION

The moderate proteinuria and high glucose levels in the urine of diabetic autoimmune NOD mice, as well as the significant loss of body weight, agreed with various other reports [7,8,10,16,21,24,25,35] that have demonstrated the usefulness of this experimental model for studying diabetes.

Microscopic examination of mice with confirmed diabetes showed atrophy of the oral epithelium, with clear cellular polymorphism and poorly-defined cell layers. The alterations seen included a reduced number of cell organelles, cell membrane disorganization, the accumulation of lipid droplets in the cytoplasm, increased intercellular space and slight superficial desquamation. In non-diabetic NOD mice, moderate morphological alterations were noted on the cheek mucosa. These changes were probably related to an autoimmune factor since these mice develop a lymphocytic infiltration of the pancreatic islets of Langerhans with concomitant beta cell destruction, resulting in the loss of insulin secretion [20]. However, pre-diabetic NOD mice represent an imperfect autoimmune model because the changes observed in the various tissues are not intense [36,41].

Elgeneidy *et al.* [9] reported a chronic inflammatory process in the connective tissue of homozygous obese mice with diabetes. Rats with chemically induced diabetes show a reduction in cell proliferation 3-4 weeks after the reported onset of the diabetic state, but with no epithelial atrophy [16]. Reuterving *et al.* [31] reported periodontal disease characterized by an inflammatory process in the oral tissue of rats with chemically induced diabetes. Similar studies in rats with two-week of diabetes showed the presence of inflammatory cells adjacent to the oral epithelium, with an inflammatory

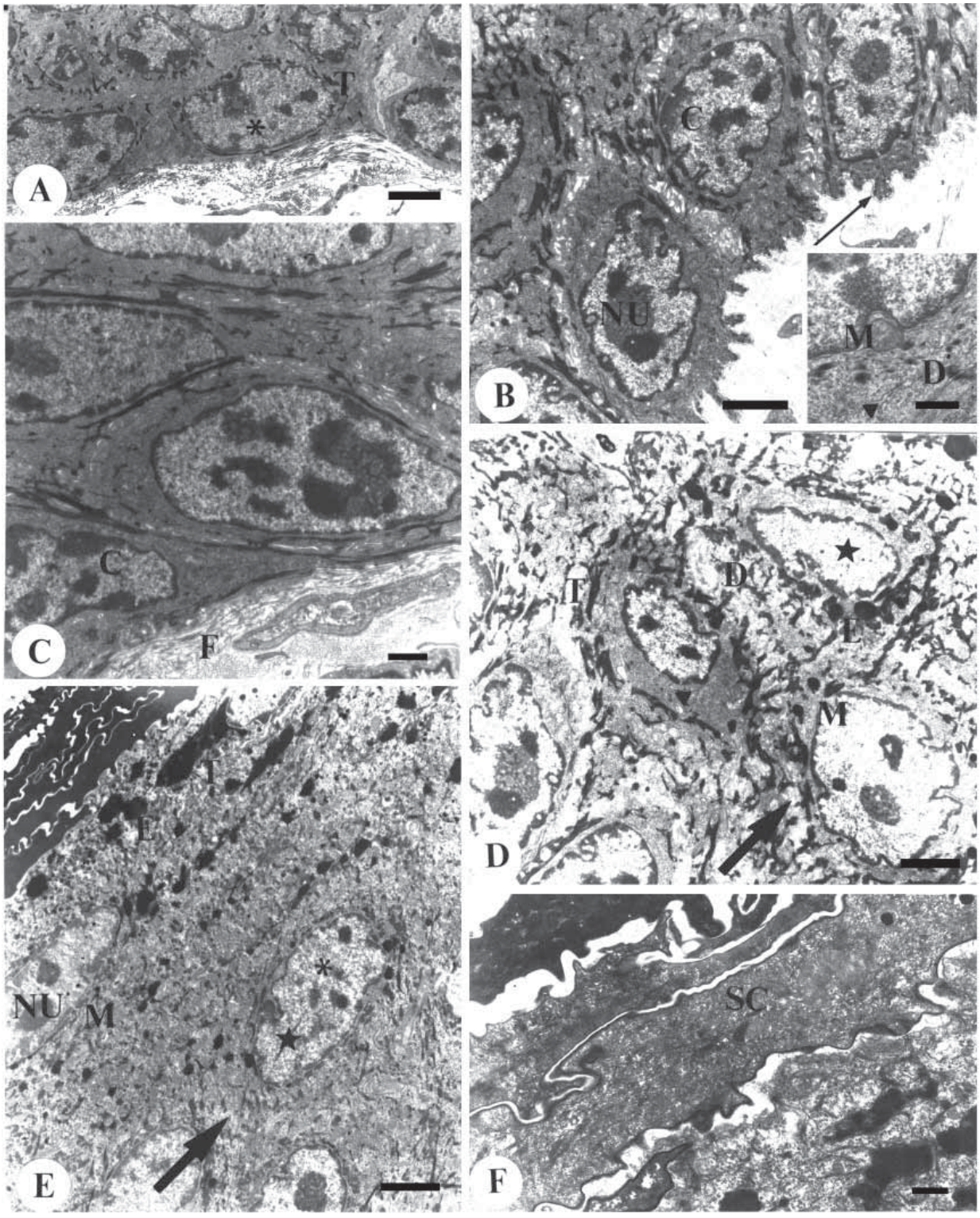


**Figure 2.** Transmission electron micrographs of the epithelial cells of Balb/c mice. **A:** Columnar basal cells (**asterisk**) and tonofilaments (**T**). Ba r= 50 µm. **B:** Intact basement membrane (**thin arrow**), nucleolus (**NU**) and condensed chromatin (**C**) close to the nuclear membrane. Bar= 50µm. **Inset:** Granular endoplasmic reticulum (**short arrow**), mitochondrion (**M**) and desmosome (**D**). Bar = 200 µm. **C:** Columnar basal cells and condensed chromatin close to the nuclear membrane (**C**). Lamina propria with collagen fibers (**F**). Ba r= 200 µm. **D:** Spinosum cell layer: nucleus (**star**), granular endoplasmic reticulum (**short arrow**), mitochondrion (**M**), electron-dense granules (**E**), tonofilaments (**T**), reduced intercellular space (**long arrow**) and desmosomes (**D**). Bar = 50 µm. **E:** Granulosum cells (**asterisk**): nucleus (**star**) and nucleolus (**NU**), mitochondria (**M**), electron-dense granules (**E**) associated with tonofilaments (**T**) and intercellular space (**long arrow**). Ba r= 50 µm. **F:** Corneum layer (SC). Bar = 200 µm.

infiltrate in connective tissue characterized by a reduced occurrence of fibroblasts and collagen and an increase in plasma cells compared to healthy animals [15,34]. In addition, Batbayar *et al.* [3] observed an increased number of mast cells associated with neurogenic inflammation and vasoconstriction in the oral mucosa of streptozotocin induced diabetic rats.

In contrast to these findings, rats with five weeks of streptozotocin-induced diabetes showed no effective inflammatory process, although there was reduced cell proliferation and reduced thickening of the epithelial lining [35]. Likewise, a study of the effects of chemically induced diabetes in rats subjected to mechanical pressure of the oral mucosa revealed no inflammatory cells or epithelial atrophy, although there was a reduced rate of cell proliferation [27]. In the rats with four weeks of experimentally induced diabetes, the cells of the oral mucosa showed accelerated DNA fragmentation and apoptosis after mechanical pressure, with reduced intercellular adhesion in the spinosum layer and early exfoliation in the corneum layer. However, the laminar arrangement and thickness of the cell layer were maintained [25]. A clinical study of cellular polymorphism suggested that the microscopic alterations produced by diabetes in the oral epithelium could be used to diagnose this disease [1]. Together, these studies show that diabetes *per se* leads to marked cellular transformations in the different layers of the cheek epithelium. In addition the morphological damage, seen here in diabetic NOD mice could be potentiated by an autoimmune factor.

NOD mice develop a lymphocytic infiltration of the pancreatic islets with concomitant beta cell destruction that results in the loss of insulin secretion and uncontrolled blood glucose levels [20]. Clinical studies have also shown that diabetic patients are susceptible to oral diseases, probably because of their reduced defense against infection and the impaired process of lesion healing caused by the suppression of collagen synthesis and excessive collagenolytic activity [14,29]. In a series of biopsies from 28 adult diabetic patients, increased periodontal disease was confirmed by the presence of chronic inflammatory cells [19]. In contrast, no significant inflammatory processes in connective tissue and no morphological changes in blood vessels were seen in biopsies from diabetic patients of different ages [23]. However, a similar study of diabetic patients of different ages revealed a high incidence of gingivitis and periodontitis, with the intensity of these diseases being directly proportional to the patient's chronological age and not to the duration of diabetes [5,6]. Barnett *et al*. [2] detected a low incidence of periodontitis in 45 young diabetic patients and suggested that it was inappropriate to relate the chronological age with the incidence of oral disease. According to Renner [30], diabetic patients who use dentures have high rates of ulceration in the supporting oral mucosa.

The structural alterations detected here confirmed the harmful effects of diabetes and showed that autoimmune diabetes impair the lining and protective functions of the epithelium in the cheek mucosa. Such modifications may alter oral homeostasis and hinder epithelial regeneration and healing, in addition, to exposing the oral mucosa to the action of infectious and carcinogenic agents.

**ACKNOWLEDGMENTS**

This work was supported by grants from CNPq (Brazilian National Council for Scientific and Technological Development), FAEP-UNICAMP (No. 1245/02) and FAPESP. We thank Prof. Stephen Hyslop, Department of Pharmacology, FCM, UNICAMP, for English revision.

## REFERENCES

1. Alberti S, Spadella CT, Francischone TRCG, Assis GF, Cestari TM, Taveira LAA (2003) Exfoliative cytology of the oral mucosa in type II diabetic patients: morphology and cytomorphometry. *J. Oral Pathol. Med*. **32**, 538-543.
2. Barnett ML, Baker RL, Yancey JM, MacMillan DR, Kotoyan M (1984) Absence of periodontitis in a population of insulin-dependent diabetes mellitus (IDDM) patients. *J. Periodontol*. **55**, 402-405.
3. Batbayar B, Somogyi J, Zelles T, Feher E (2003) Immunohistochemical analysis of substance P-containing nerve fibres and their contacts with mast cells in the diabetic rat's tongue. *Acta Biol. Hung*. **54**, 275-283.
4. Cagnon VHA, Camargo AM, Rosa RM, Fabiani R, Padovani CR, Martinez FE (2000) Ultrastructural study of the ventral lobe of the prostate of mice with streptozotocin induced diabetes (C57BL/6J). *Tissue Cell* **32**, 275-283.

**Figure 3.** Transmission electron micrographs of non-diabetic NOD mice. **A:** Basal cells (**asterisk**), tonofilaments (**T**), lipid droplet (**thick arrow**) and lamina propria with collagen fibers (**F**). Ba r= 50 μm. **B:** Basement membrane (**thin arrow**), mitochondrion (**M**), granular endoplasmic reticulum (**short arrow**) and tonofilaments (**T**). Condensed chromatin (**C**) close to the nuclear membrane. Bar = 200 μm. **Inset:** Desmosomes (**D**). Ba r = 200 μm. **C:** Nuclear deformity, showing marked granular endoplasmic reticulum (**arrow**), tonofilaments (**T**), nucleolus (**NU**), condensed chromatin (**C**) close to the nuclear membrane, intercellular space (**long arrow**) and the lamina propria with collagen fibers (**F**). Bar = 200 μm. **D:** Cells of the spinosum layer containing a nucleus (**star**), mitochondria (**M**), electron-dense granules (**E**), tonofilaments (**T**), desmosomes (**D**), condensed chromatin (**C**) close to the nuclear membrane and intercellular space (**curved arrow**). Bar = 50 μm. **E:** Granulosum cells with the nucleus (**star**), keratohyalin-like electron-dense granules (**E**) associated with tonofilaments (**T**), and intercellular space (**long arrow**). Bar = 50 μm. **F:** Corneum cells showing desquamation (**SC**). Bar = 200 μm.

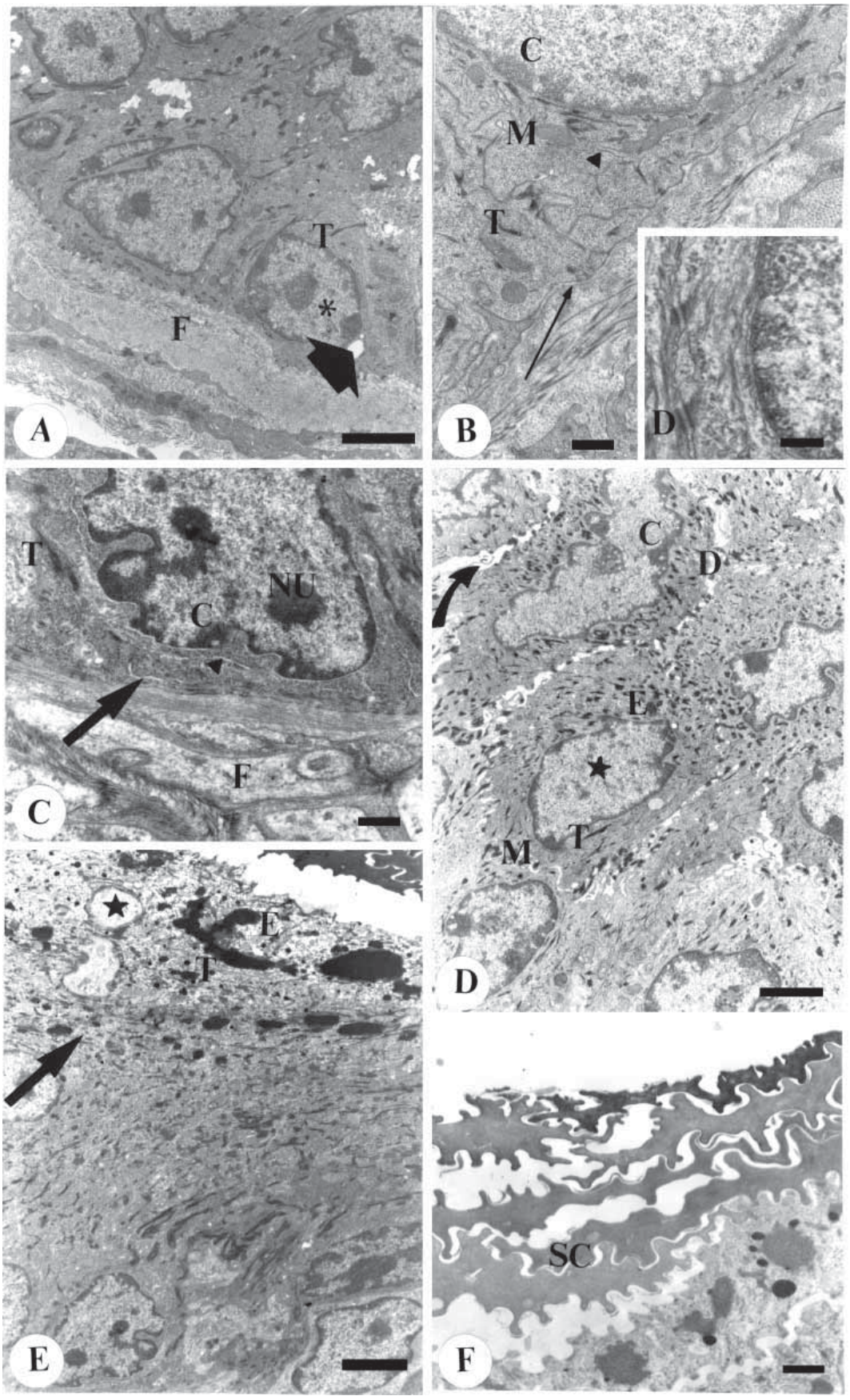
A
T
F
*
B
C
M
T
D
C
T
NU
C
F
D
C
D
E
M
T
E
T
E
F
SC

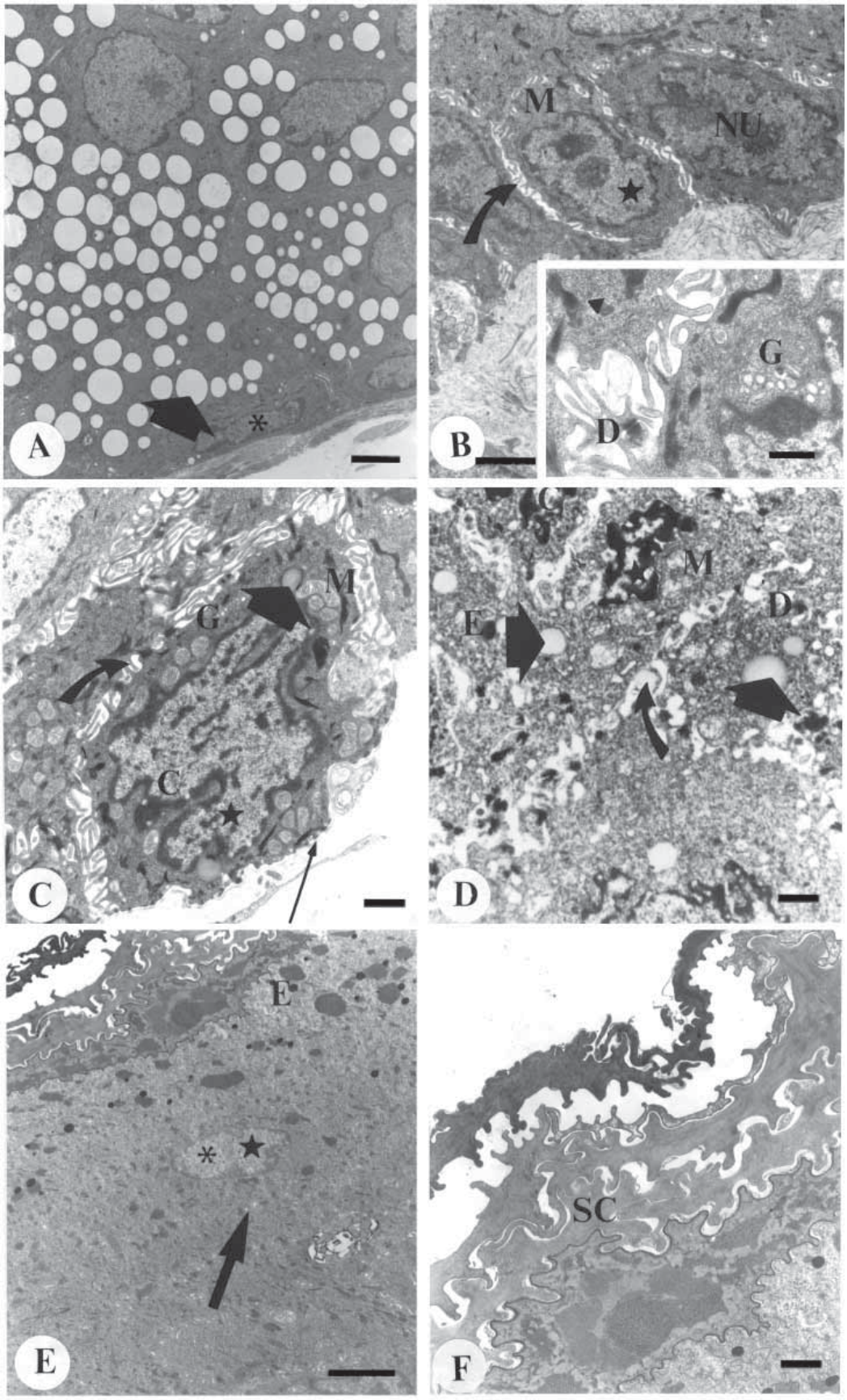
A
B
M
NU
G
D
C
M
G
C
D
M
E
D
E
E
SC
F

5. Cianciola LJ, Park BH, Bruck E, Mosovichand L, Genco RJ (1982) Prevalence of periodontal disease in insulin-dependent diabetes mellitus (juvenile diabetes). *J. Am. Dent. Assoc*. **104**, 653-660.
6. Cohen DW, Friedman LA, Shapiro J, Kyle GC, Franklin S (1970) Diabetes mellitus and periodontal disease: two-year longitudinal observations. Part I. *J. Periodontol*. **41**, 709-718.
7. Conget I (2002) Diagnosis, classification and cathogenesis of diabetes mellitus. *Rev. Esp. Cardiol*. **55**, 528-538.
8. Daubresse JC, Meunier J, Wilmotte AS, Luickx AS, Lefebvre PJ (1978) Pituitary-testicular axis in diabetic men with and without sexual impotence. *Diab. Metab*. **4**, 233-237.
9. Elgeneidy K, Stallard RE, Fillios LC, Goldman HM (1974) Periodontal and vascular alterations: their relationship to the changes in tissue glucose and glycogen in diabetic mice. *J. Periodontol*. **45**, 394-401.
10. El-Salhy M, Zachrisson S, Spangéus A (1998) Abnormalities of small intestinal endocrine cells in non-obese diabetic mice. *J. Diab. Complicat.* **12**, 215-223.
11. Fushini H (1980) The effect of parabiosis on serum and kidney glycosidase activities in spontaneous diabetic mice. *Diabetologia* **19**, 50-53.
12. Gomes I, Cagnon VHA, Carvalho CAF, De Luca IMS (2002) Stereology and ultrastructure of the seminal vesicle of C57/BL/6J mice following chronic alcohol ingestion. *Tissue Cell* **34**, 177-186.
13. Gomori G, Goldner MG (1943) Production of diabetes mellitus in rats with alloxan. *Proc. Soc. Exp. Biol. Med*. **54**, 287-290.
14. Grossi SG, Skrepcinski FB, DeCaro T, Zambon JJ, Cummins D, Genco RJ (1996) Response to periodontal therapy in diabetics and smokers. *J. Periodontol*. **71**, 1094-1102.
15. Györfi A, Fazekas Á, Fehér E, Ender F, Rosivall L (1996) Effects of streptozotocin-induced diabetes on neurogenic inflammation of gingivomucosal tissue in rat. *J. Periodontol. Res*. **31**, 249-255.
16. Hamilton AI, Blackwood HJJ (1977) Insulin deficiency and cell proliferation in oral mucosal epithelium of the rat. *J. Anat*. **124**, 757-763.
17. Ho SM (1990) Prostatic androgen receptor and plasma testosterone level in streptozotocin-induced diabetic rats. *J. Steroid. Biochem. Mol. Biol*. **38**, 67-72.
18. Homo-Delarche F (2001) Is pancreas development abnormal in the non-obese diabetic mouse, a spontaneous model of type I diabetes? *Braz. J. Med. Biol. Res*. **34**, 437-447.
19. Hove K, Stallard RE (1970) Diabetes and the periodontal patient. *J. Periodontol*. **41**, 713-718.
20. Humphreys-Beher MG, Yamachika S, Yamamoto H, Maeda N, Nakagawa Y, Peck A B, Robinson CP (1998) Salivary gland changes in the NOD mouse model for Sjögren's syndrome: is there a non-immune genetic trigger? *Eur. J. Morphol*. **36**, 247-251.
21. Hunt EL, Bailey DW (1961) The effects of alloxan diabetes on the reproductive system of young male rats. *Acta Endocrinol*. **38**, 432-440.
22. Karnovsky JMA (1965) Formaldehyde-glutaraldehyde fixative in high osmolarity for use in electron microscopy. *J. Cell Biol*. **27**, 137a-138a.
23. Listgarten MA, Ricker FH, Laster L, Shapiro J, Cohen DW (1974) Vascular basement lamina thickness in the normal and inflammed gingiva of diabetics and non-diabetics. *J. Periodontol*. **45**, 676-684.
24. Makino S, Kunimoto K, Muraoka Y, Mizushima Y, Katagiri K, Tochino Y (1980) Breeding of nonobese. *Diabet. Strain Mice* **1**, 1-13.
25. Maruo Y, Sugimoto T, Oka M, Hara T, Sato T (2001) Accelerated DNA fragmentation of the denture-bearing epithelium in an animal model of diabetes. *J. Oral Rehabil*. **28**, 393-399.
26. Montgomery DC (1991) *Design and Analysis of Experiments*. John Wiley: New York.
27. Mori S, Sato T, Hara H, Shirai Y, Maruo Y, Minagi S (1999) The effect of diabetes mellitus on histopathological changes in the denture–supporting tissues under continuous mechanical pressure in rat. *J. Oral Rehabil*. **26**, 80-90.
28. Norman GR, Streiner DL (1994) *Biostatistics: The base essentials*. C.V. Mosby: St. Louis.
29. Prichard JF (1966) *Advanced Periodontal Disease: Surgical and Prosthetic Management.* W.B. Saunders: Philadelphia.
30. Renner RP (1981) *Diagnosis and treatment planning*. In: *Complete Dentures: a Guide for Patient Treatment*. (Renner, RP, ed). pp. 1-63. Masson Publishing USA: New York.
31. Reuterving CO, Hägg E, Gustafson GT (1986) Root surface caries and periodontal disease in long-term alloxan diabetic rats. *J. Dent. Res*. **65**, 689-694.
32. Reynolds ES (1963) The use of lead citrate at high pH as an electron-opaque stain in electron microscopy. *J. Cell Biol*. **71**, 208-212.
33. Robbins SL (1989) Systemic diseases. Diabetes Mellitus: Structural and Functional Pathology. In: *Pathologic Basis of Disease.* (Robbins SL, ed). pp. 992-1010. W.B. Saunders Company: Montreal.
34. Seppala B, Sorsa T, Ainamo J (1997) Morphometric analyses of cellular and vascular changes in gingival connective tissue in long-term insulin-dependent diabetes. *J. Periodontol*. **68**, 1237-1245.
35. Shirai H, Sato T, Hara T, Minagi S (1998) The effect of diabetes mellitus on histopathological changes in the tissues under denture base and without mechanical pressure. *J. Oral Rehabil*. **25**, 715-720.
36. Spangeus A, Forsgren S, El-Salhy M (2001) Effect of diabetic state on co-localization of substance P and serotonin in the gut in animal models. *Histol. Histopathol*. **16**, 393-398.
37. Stefan SF (1996) Definition and classification of diabetes including maturity-onset diabetes of the young. In: *Diabetes Mellitus: a Fundamental and Clinical Text.* (Stefan SF, ed). pp. 251-295. W. B. Saunders: Philadelphia.
38. Tochino Y (1987) The NOD mouse as model of type I diabetes. *CRC Crit. Rev. Immunol*. **8**, 49-81.
39. Watson ML (1958) Staining of tissue sections for electron microscopy with heavy metals. *J. Biophys. Biochem. Cytol*. **4**, 727-730.
40. Weibel ER (1979) Stereological principles for morphometry in electron microscopic cytology. *Int. Rev. Cytol*. **26**, 235-302.
41. Yamano S, Atkinson JC, Baum BJ, Fox PC (1999) Salivary gland cytokine expression in NOD and normal Balb/c mice. *Clin. Immunol*. **92**, 265-275.

Received: September 22, 2004
Accepted: November 19, 2004

**Figure 4.** Transmission electron micrographs of diabetic NOD mice. **A:** Atypical basal cells (**asterisk**) and lipid droplets (**thick arrow**). Ba r = 50 µm. **B:** Increase in the intercellular space (**curved arrow**), mitochondria (**M**), nucleus (**star**) and nucleolus (**NU**). Bar = 50 µm. **Inset:** Basal cell layer: granular endoplasmic reticulum (**arrowhead**), Golgi complex (**G**) and desmosomes (**D**). Bar = 200 µm. **C:** Basal cell layer: Increased intercellular space (**curved arrow**), lipid droplets (**thick arrow**), mitochondria (**M**), nucleus (**star**), condensed chromatin (**C**) close to the nuclear membrane and Golgi complex (**G**). Bar = 200 µm. **D:** Spinosum cells with lipid droplets (**thick arrows**), irregular nucleus (**star**), condensed chromatin (**C**) close to the nuclear membrane, mitochondrion (**M**), electron-dense granule (**E**), intercellular space (**curved arrow**) and desmosomes (**D**). Bar = 200 µm. **E:** Granulosum cell (**asterisk**), with nucleus (**star**), electrondense granules (**E**) and intercellular space (**long arrow**). Bar = 50 µm. **F:** Minor desquamation of the corneum layer (**SC**). Bar = 200 µm.